The Modified Palmer Drought Severity Index Based on the NCEP North American Regional Reanalysis

KINGTSE C. MO AND MUTHUVEL CHELLIAH

NOAA/NWS/NCEP Climate Prediction Center, Camp Springs, Maryland

(Manuscript received 29 August 2005, in final form 2 February 2006)

ABSTRACT

A 32-km high-resolution modified Palmer drought severity index (MPDSI) based on the National Centers for Environmental Prediction (NCEP) North American Regional Reanalysis (RR) from 1979 to 2004 is presented. The assumptions of Palmer, such as the water balance equation, the difference between observed precipitation and the climatologically expected precipitation over the maximum conditions, and the changes of the index as a function of the current index, are preserved. Many deficiencies of the original PDSI are eliminated by taking fields directly from the RR or by making better estimates. For example, fields such as potential evapotranspiration, evaporation, runoff, total soil moisture, and soil moisture change in a given month are obtained directly from the RR. The potential recharge is defined as the total soil moisture needed to reach the maximum total soil moisture at each grid point for each calendar month. The potential precipitation is defined as the maximum precipitation at each grid point for a given calendar month. The underground volumetric soil moisture includes both frozen and liquid form. Therefore, the contribution of snowmelt is taken into account inexplicitly. The questionable assumptions of two-layer soil model and the available soil moisture capacity are no longer needed. Overall, the MPDSI, when averaged over a large area and long time, often resembles the traditional PDSI based on the Palmer formula and the climate-division data. The MPDSI obeys Gaussian distribution, and so it can also be used to assess the potential for floods. Together with a consistent suite of soil moisture, surface energy, and atmospheric terms from the RR, the MPDSI can be used to monitor and diagnose drought and floods.

1. Introduction

In 2003, the Western Governor's Association and the National Oceanic and Atmospheric Administration (NOAA) recognized the need to have a better drought monitoring and forecast system for the United States. A drought early warning system would help to mitigate the impacts of drought on the U.S. economy, including human suffering and property losses. One way to establish drought warning is to monitor and forecast indices that incorporate the long-term changes in precipitation and hydrological conditions.

There are two indices commonly used to monitor drought: the standardized precipitation index (SPI) and the Palmer drought severity index (PDSI). The relatively simple SPI is based exclusively on precipitation (Hayes et al. 1999) and has been used to monitor drought at the National Drought Mitigation Center and the Western Regional Climate Center (McKee et al. 1993, 1995). It is flexible and can be applied to monitor droughts as well as floods on different time scales. The PDSI, however, is based on the water balance between soil moisture supply and demand (Palmer 1965). The Climate Prediction Center and the National Climatic Data Center (NCDC) have routinely produced the PDSI based on the U.S. climate-division data that are available from the NCDC from 1895 to the present. This dataset is labeled as the PDSI(ncdc) in this study.

Some of the rules used to establish the PDSI are arbitrary (Alley 1984). Palmer (1965) calibrated most parameters based on limited temperature and precipitation records of a few stations over the Great Plains from the 1930s to the 1960s. The five major shortcomings of the PDSI are as follows.

1) The potential evapotranspiration (PE) is estimated based on the formula derived by Thornthwaite (1948). It is a function of surface temperature alone. It will be shown later that this estimation differs

Corresponding author address: Kingtse Mo, Climate Prediction Center/NCEP/NWS, 5200 Auth Rd., Camp Springs, MD 20746.
E-mail: kingtse.mo@noaa.gov

from the estimation adopted in the National Centers for Environmental Prediction (NCEP) regional reanalysis by as much as 60%.
2) For lack of observations or better data, Palmer (1965) assumed that there are only two soil layers and that the available water capacity (AWC) is fixed at a constant 254 mm over the entire United States. In reality, however, the AWC is regionally dependent and is a function of soil type and soil properties (Schaake et al. 2004; Robock et al. 2003; Cosby et al. 1984).
3) Over the western region, all winter precipitation is treated as rain; therefore, the snowmelt and frozen groundwater are not taken into account.
4) Most parameters used in the PDSI are sensitive to calibration (Karl 1983, 1986; Mintz and Walker 1993; Wells et al. 2004). Over the contiguous United States, precipitation and temperature have increased in the twentieth century (Groisman et al. 2004). The linear trend of the area-averaged temperature based on the U.S. Historical Climatology Network for the period of 1895–2002 is 0.56°C (100 yr)$^{-1}$. The trends are regionally dependent, with warming over the West and weaker cooling over the Southeast. Their study also shows that the mean total and heavy precipitation events increased during the past three decades. Therefore, parameter calibrations based on data in the 1960s or 1970s may not be appropriate for the current period. Calibrations should be based on the entire data period.
5) The potential precipitation is assumed to be the same as AWC. In reality, there is no relationship between precipitation and AWC (Alley 1984).

Because of the recent success of the North American Land Data Assimilation System (NLDAS; Mitchell et al. 2004) and the land surface model (LSM) activities (Ek et al. 2003), there is no need to estimate parameters used in the PDSI. The NLDAS/LSM is also a subcomponent of the North American Regional Reanalysis (Mesinger et al. 2006), and continues as the Regional Climate Data Assimilation System from 1979 to the present. The entire dataset is labeled as the RR. Both verification and intercomparison studies indicate that the hydrological cycle over the United States depicted by the RR is realistic (Mo et al. 2005; Fan et al. 2006).

The goal of this paper is to present a modified high-resolution PDSI to monitor droughts and floods over the United States based on the RR. Because the PDSI has been widely used in the operational and research community, we would like to preserve the original framework of Palmer (1965). The new modified Palmer drought severity index (MPDSI) adopts two pieces from the original framework of Palmer (1965), as follows.

1) The PDSI is based on the water balance equation and the difference between the actual precipitation and the climatological estimation of precipitation under the maximum conditions, which Palmer labeled as "climatically appropriate for existing conditions" (CAFEC).
2) The PDSI obeys a first-order differential equation: the change of the PDSI is proportional to the PDSI at that time.

The PDSI(ncdc) is based on the climate-division data. The coarse-resolution data may not be able to take into account the elevation-dependent changes. To monitor drought or floods over the western mountain region, a high-resolution PDSI based on the 32-km RR is desirable. Many fields needed to calculate the PDSI such as evaporation, potential evapotranspiration, total soil moisture, soil moisture change, and runoff are obtained directly from the RR. They are self consistent. Many shortcomings of the PDSI listed above can be corrected.

The procedures to compute the MPDSI are outlined in section 2. The normalization procedures proposed by Palmer (1965) will be modified. The comparison with the PDSI(ncdc) and SPI is given in section 3. Conclusions are given in section 4.

2. The MPDSI

a. The regional-reanalysis products

The NCEP regional-reanalysis model is the NCEP operational Eta Model version of 2003. The horizontal grid spacing is 32 km, and there are 45 layers in the vertical direction (Mesinger et al. 2006). The data are archived on the Eta Advanced Weather Interactive Processing System grid, and this grid is used for the MPDSI. The RR has the "Noah" LSM as a subcomponent. The description of the Noah LSM and evaluation can be found in Ek et al. (2003) and Mitchell et al. (2004). In the Noah LSM, there are four soil layers. It has improvements to surface runoff and infiltration (Schaake et al. 1996), bare soil evaporation, vegetation phenology (Betts et al. 1997), and surface thermal roughness length (Chen et al. 1996, 1997). The evapotranspiration is the sum of transpiration from the plant canopy, bare soil evaporation, and direct evaporation of canopy intercepted water (Chen et al. 1996, Betts et al. 1997). From 1997 onward, the bare soil evaporation is based on Mahfouf and Noilhan (1991) with a modification to take into account the large gradients in soil moisture near the surface (Ek et al. 2003). For the cold

season, the new snowpack and frozen soil physics improve the low-level temperature and surface heating (Ek et al. 2003; Koren et al. 1999).

Input data for the RR were discussed in Shafran et al. (2004) and Mesinger et al. (2006). One important aspect of the RR is that the RR assimilates precipitation over the United States and Mexico. Over land, the major precipitation data source is the daily rain gauge data interpolated to a 1° grid using a Cressman scheme (Cressman 1959). This dataset covers the United States and Mexico (Higgins et al. 2000). Over the United States, precipitation P also has the Parameter-Elevation Regressions on Independent Slopes Model (PRISM) adjustment. Therefore, P is more realistic over the western mountains. The intercomparison and evaluation of the Noah LDAS and other LDAS products can be found in Robock et al. (2003), Lohmann et al. (2004), and Schaake et al. (2004). Fan et al. (2006) intercompared soil moisture products from many LDAS and simple models.

b. Precipitation deviation from the CAFEC

In this paper, the MPDSI is based on monthly means of the RR products for the base period from 1979 to 2004. The long-term monthly means and maxima are calculated using data from the same base period. The same definition and procedures can be applied to other time scales and to any NLDAS products. As with the Palmer (1965) model, the MPDSI estimates the departure of P from the CAFEC:

$$d = P - \text{CAFEC}, \quad \text{where} \tag{1}$$

$$\text{CAFEC} = \alpha\text{PE} + \beta\text{PR} + \gamma\text{PRO} - \delta\text{PL}, \tag{2}$$

PE is the potential evapotranspiration, PR is the potential recharge, PRO is the potential runoff, and PL is the potential soil moisture loss defined as the soil moisture loss when there is no P. These are measurements of maximum conditions that could exist.

The coefficients α, β, γ, and δ are means for each month averaged over the base period. For example,

$$\alpha = \overline{\text{ET}}/\overline{\text{PE}}, \tag{3}$$

where ET is the evapotranspiration and the overbar denotes the long-term monthly mean from 1979 to 2004. In a similar way, β is the ratio of mean recharge divided by mean potential recharge PR, γ is the ratio of mean runoff divided by mean potential runoff PRO, and δ is the ratio of mean moisture loss divided by mean potential moisture loss PL.

Palmer (1965) estimated PE based on Thornthwaite's (1948) formula, which is a function of surface temperature only. The MPDSI uses the PE from the RR. There are large differences between the two (Fig. 1). Both PEs capture the seasonal cycle. Large values extend northward from winter to summer and reach a maximum in July and then retreat southward from summer to winter. The maximum is located over the Southwest. However, the PE based on the Thornthwaite formula is weaker than the RR and lacks the strong east–west contrast. The mean PE from the RR shows large values over the West and the Southwest, with two maxima located over western Texas and California, respectively. In July, the maximum of PE from RR is about 12 mm day^{-1} located in California, whereas the maximum from the Thornthwaite formula is only 5 mm day^{-1}.

Monthly mean ET, runoff, soil moisture recharge, soil moisture loss, and total soil moisture at the beginning of the month are taken directly from the RR archive. The RR has four layers of soil, and the total thickness is 200 cm. The total soil moisture includes both liquid and frozen form from the ground surface down to 200-cm depth. The potential recharge PR is defined as the soil moisture needed to bring soil to the total soil moisture maximum, taken to be the maximum of the total soil moisture from 0 to 200 cm ($S_{\max}$) at each grid point for each calendar month calculated from the base record.

The potential recharge PR for each month is defined as

$$\text{PR} = S_{\max} - S', \tag{4}$$

where S' is the total soil moisture at the beginning of the month. The potential soil moisture loss PL is taken as

$$\text{PL} = \min(\text{PE}, S'). \tag{5}$$

Palmer (1965) assumed that the potential precipitation is equal to AWC; thus, the potential runoff PRO = S' or the difference between AWC and PR. The problem with this formulation is that there is no relationship between P and AWC. Precipitation depends on the vertically integrated moisture convergence and evaporation. The moisture fluxes are calculated from the atmospheric circulation. They are available from the RR, but they are generally absent from most NLDAS products. The MPDSI should be applied to the NLDAS as well as the RR. Therefore, the potential precipitation is taken as the maximum precipitation $P_{\max}$ at each grid point for each calendar month. The potential runoff is the difference between the maximum precipitation and the potential recharge:

$$\text{PRO} = P_{\max} - \text{PR}. \tag{6}$$

There is no need to use the two soil layers and the AWC. This approach addresses many concerns of the original PDSI.

CAFEC and d were calculated for each month from

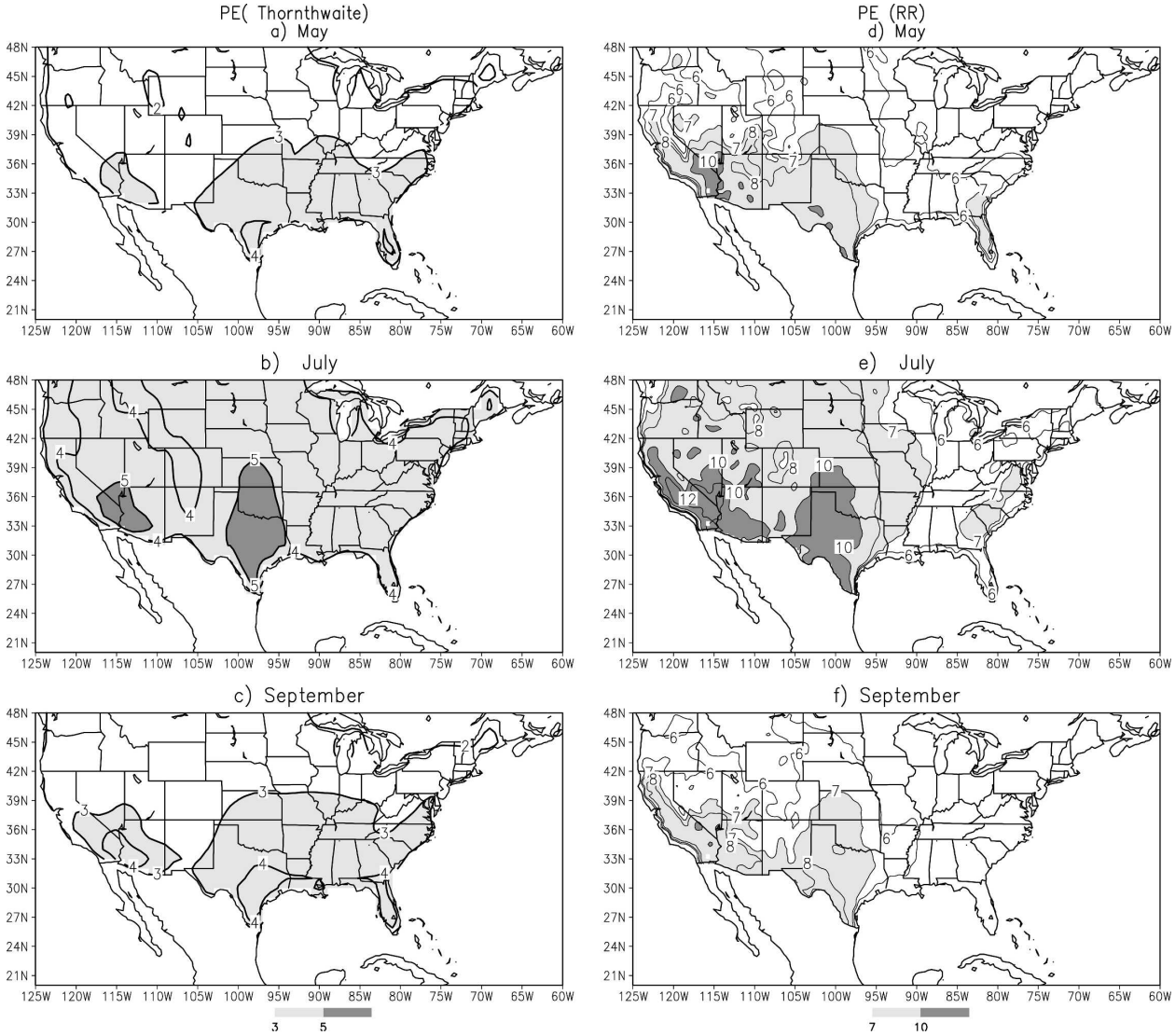

FIG. 1. The evapotranspiration (PE) for (a) May, (b) July, and (c) September averaged for the period of 1979–2004 based on the Thornthwaite formula. Contour interval is 1 mm day^{-1}. Values greater than 3 (5) mm day^{-1} are shaded light (dark), (d)–(f) Same as (a)–(c), but from the RR. Values greater than 7 (10) mm day^{-1} are shaded light (dark).

1979 to 2004 using the equations listed above. To update the MPDSI, the maxima and long-term means should be calculated using the same base period to assume that the long-term mean of d averaged over the base period is close to zero. To be able to compare the MPDSI over different regions and months, normalization is needed.

c. Normalization: Procedures and calibration

To take into account regional differences, d is weighted by a factor K:

$$Z = dK, \tag{7}$$

where Z is called the moisture anomaly index. Palmer (1965) obtained K empirically based on stations in Iowa and Kansas under drought conditions. He defined calibration factor K for each month i as

$$K(i) = K'(i)\left[\frac{\text{const1}}{\sum_{i=1}^{12} \overline{D(i)K'(i)}}\right], \quad \text{where} \tag{8}$$

$$K'(i) = 1.5 \log\left[\left(\frac{\overline{\text{PE} + R + \text{RO}}}{\overline{P + L}} + 2.8\right)_i \Big/ \overline{D(i)}\right] + 0.5, \tag{9}$$

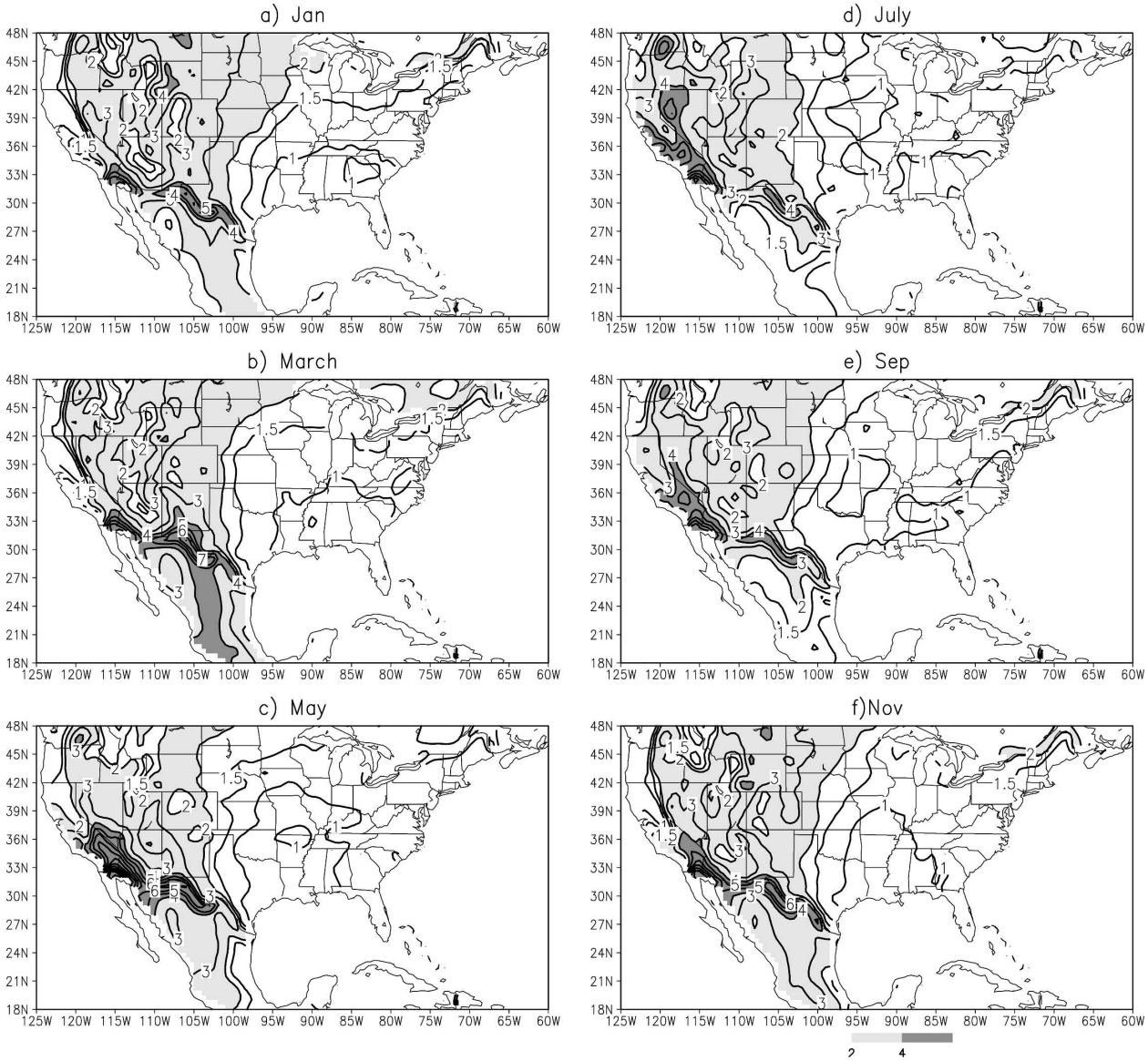

FIG. 2. The normalization factor K calculated based on Palmer (1965) for (a) January, (b) March, (c) May, (d) July, (e) September, and (f) November. Contour interval is 1 dimensionless unit, with contour 1.5 added. Values greater than 2 are shaded.

where R is the recharge, RO is the runoff, L is the moisture loss, P is precipitation, and $D(i)$ is the monthly mean of the absolute values of d for month i. The overbar denotes the mean for the base period. Palmer estimated const1 = 17.67 as the normalization factor based on the sum

$$\sum_{i=1}^{12} \overline{D(i)K'(i)}$$

averaged over nine stations over the Great Plains during drought conditions.

The K factors for selected months based on Eqs. (8) and (9) using the RR data are given in Fig. 2. There is a large east–west contrast. The K values are near 1 over the central and eastern United States. Large values are located over the western United States, with maxima of approximately 5–6 near the boundary between the United States and Mexico. Over the mountains, the influence of orography is apparent. The K estimated this way is qualitatively consistent with the estimate given by Karl (1983, his Fig. 3) using state temperature and precipitation data from 1885 to 1981. The most striking feature is that there is very little seasonal dependence.

The weak seasonal dependence of K allows us to

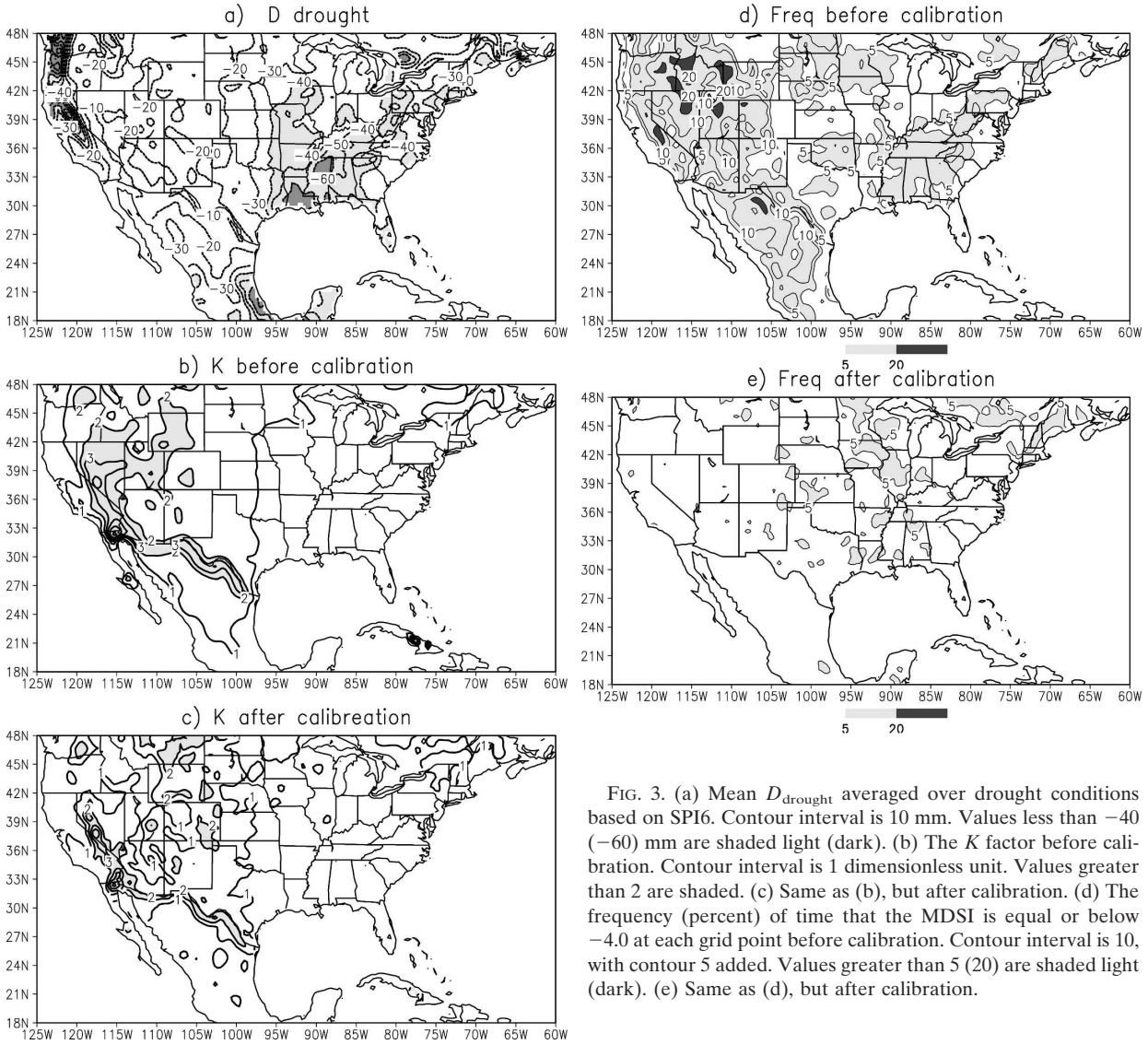

FIG. 3. (a) Mean D_{drought} averaged over drought conditions based on SPI6. Contour interval is 10 mm. Values less than −40 (−60) mm are shaded light (dark). (b) The K factor before calibration. Contour interval is 1 dimensionless unit. Values greater than 2 are shaded. (c) Same as (b), but after calibration. (d) The frequency (percent) of time that the MDSI is equal or below −4.0 at each grid point before calibration. Contour interval is 10, with contour 5 added. Values greater than 5 (20) are shaded light (dark). (e) Same as (d), but after calibration.

pool all data together. If $K'(i)$ is independent of i, Eq. (8) can be written as

$$K = \frac{\text{const2}}{D_{\text{drought}}}, \tag{10}$$

where D_{drought} is the sum of d for months under drought conditions. Therefore, D_{drought} can be estimated as the composite of d at each grid point during droughts, and const2 is the normalization constant; K can be applied to all months.

To identify a drought, the SPI for 6-month mean precipitation (SPI6) was used. SPI6 from 1948 to 2004 was computed using the gauge-based P analysis (Higgins et al. 2000). That is the same dataset used in the RR data input. The longer dataset gives more stable results. The criterion for drought is when the SPI6 is less than −1 (McKee et al. 1993, 1995). We formed the composite D_{drought} at each grid point by averaging d for months for which the SPI6 is below −1. The D_{drought} map shows large negative values over the central United States and the Pacific Northwest and small negative values over the western and mountain areas (Fig. 3a). Following the method of Palmer (1965), we set K equal to 1 over the central and eastern United States (32°–48°N, 75°–100°W) to obtain the normalization constant const2 = −39.76. Then K can be obtained at each grid point from Eq. (10) (Fig. 3b). The pattern of K obtained this way is similar to the K factors from Fig. 2. They all show a strong east–west contrast. As noted earlier, large values of K are located over the

western mountain region, with maxima between the Southwest and Mexico.

Moisture anomaly index Z can be obtained from Eq. (7). After obtaining Z, the MPDSI is defined in the same way as Palmer (1965):

$$\text{MPDSI}_i = \text{MPDSI}_{i-1} + Z(i)/3 - c\text{MPDSI}_{i-1}$$

or

$$\text{MPDSI}_i = (1 - c)\text{MPDSI}_{i-1} + Z(i)/3, \qquad (11)$$

where c is a constant. Equation (11) indicates that the change of PDSI is proportional to PDSI. Therefore, $(1 - c)$ can be estimated by the autocorrelation at lag 1. We calculated $(1 - c)$ at each grid point by pooling all data together, and it had values between 0.83 and 0.94, which is close to Palmer's 0.897. For simplicity, Palmer's original value $c = 0.103$ is used.

The MPDSI obtained this way has the mean equal to zero and obeys the normal distribution. However, the range of values may not necessarily be between −4 and 4 as Palmer (1965) had defined. Figure 3d plots the frequency (percentage of months) at which the MPDSI shows an extreme drought at each grid point (MPDSI equal to or less than −4). Over the central and eastern regions, the percentage is less than 5%. However, over the western mountain region and northern Mexico, the percentage is about 10%–20%, which is too high. Wells et al. (2004) suggested that the extreme MPDSI values should be within 2% (98%) of the distribution. Therefore, the calibration suggested by Wells et al. (2004) is needed. The MPDSI calculated above serves only as the first estimate.

Based on the first estimate of the MPDSI, the calibration factor K is adjusted to require that the percentile of extreme events be within 2% (98%). The extreme events are defined as PDSI below −4 (above +4) for dry (wet) cases. After obtaining the new K factor, we then calculated the Z and MPDSI again based on the new K.

Wells et al. (2004) calibrated each climate division separately. Our record is too short to obtain a stable distribution function at each grid point to calibrate K. Here, the regional differences have already been taken into account through the D_{drought} term, which allows us to pool all grid points together. We request that the frequency of extreme drought over the United States (30°–48°N, 60°–125°W over land) is close to 2% to obtain the new K factor (Fig. 3c). The comparison between the K factors before (Fig. 3b) and after calibration (Fig. 3c) indicates that the patterns are similar, and both show large east–west contrast. Both K factors are near 1 over the central and eastern United States and are larger than that over the western mountain regions. The K after calibration shows smaller values over the western region. Maxima are still located over the boundary of the United States and Mexico, but the values are smaller. After calibration, the frequency of extreme dry events is less than 5% over most areas (Fig. 3e), down from 10%–20% before calibration (Fig. 3d).

The K factor is not sensitive to the SPI used after calibration. The D_{drought} and K factor are computed based on SPI6 (Figs. 3a,b). If the SPI for 12-month mean precipitation (SPI12) time series is used instead of SPI6, the first estimated pattern for D_{drought} is similar, and values and const2 are both smaller. After calibration following the same procedures listed above, the K factor based on SPI12 (not shown) is very similar to the K factor based on SPI6. This result indicates that the calibration decreases the spatial uncertainties of K. The new normalization procedures are simple and are based on grid points rather than a few stations. The new K factor (Fig. 3c) then was used to renormalize Z [Eq. (7)], and the final MPDSI can be recalculated from Eq. (11).

3. MPDSI in comparison with the PDSI(ncdc) and SPI

Palmer (1965) calibrated the PDSI during drought conditions, but he expected that the index is also representative for floods. The distribution function for MPDSI can be obtained by pooling all months and grid points over the United States together (Fig. 4a). The distribution is Gaussian. We also computed separate distribution functions using data over different regions—for example, the western region (west of 100°W) and eastern region (east of 100°W). The distribution functions for both regions are Gaussian, which implies that the MPDSI can be used to monitor floods as well as droughts.

Figure 4b shows the correlation between MPDSI and PDSI(ncdc) for the period from 1979 to 2004 with all months pooled together. The PDSI(ncdc) is from 344 U.S. climate divisions, and the MPDSI is on the RR grid. To compute correlation, MPDSI was interpolated to the center point of each climate division before calculating the correlation. This approximation may lower the correlations. For most places, the correlation is above 0.6. Values lower than 0.6 (shaded) are located over the Ohio Valley, Tennessee, western Montana, and along the coasts. Some differences are due to the differences in P. The 3-month means of P follow a normal distribution. We calculated correlation between 3-month P means from the climate divisions and the corresponding P from the RR interpolated to the center point of each climate division (Fig. 4c). Again, the correlation is above 0.6 except for the shaded regions. There is a remarkable correspondence between the two

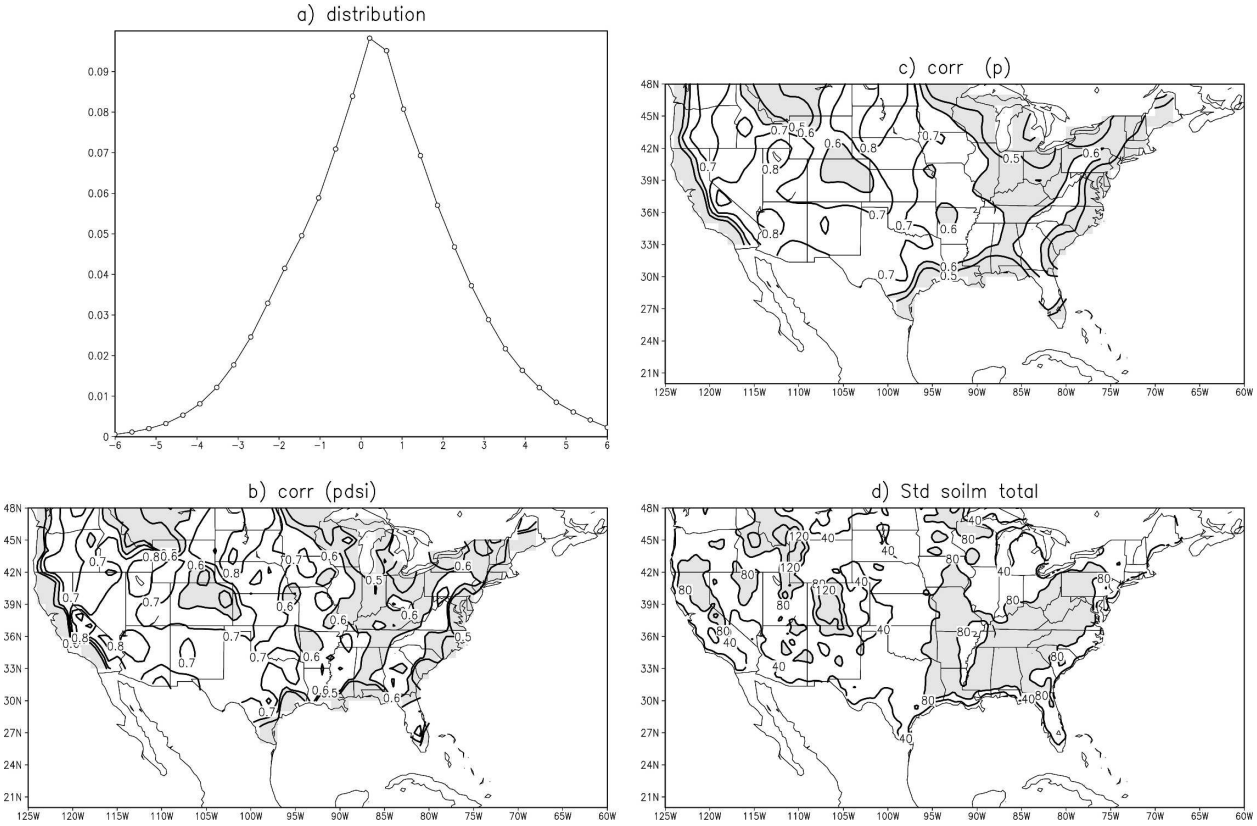

FIG. 4. (a) Distribution function of the MPDSI with all data pooled together. (b) Correlation between the MPDSI and PDSI(ncdc) for the period of 1979–2004. Contour interval is 0.1. Values less than 0.6 are shaded. (c) Same as (b), but for the correlation between *P* from the RR and *P* from the climate divisions. (d) Standard deviation of the total soil moisture. Contour interval is 40 mm. Values greater than 80 mm are shaded.

correlation maps (Figs. 4b,c). Low correlations between the MPDSI and PDSI(ncdc) occur mostly over the regions in which the correlations between the *P* datasets are themselves low. In addition to *P*, soil moisture has a larger contribution to the MPDSI than to the PDSI(ncdc) because soil conditions are not directly used in calculating PDSI(ncdc). Figure 4d shows the standard deviation of monthly mean total soil moisture for all months together. Large values are over the mountain regions during the winter months. These regions (shaded) are the areas for which soil moisture has larger contribution to the MPDSI.

Figure 5 shows the comparison between the MPDSI (plus signs) and the PDSI(ncdc) (solid line) averaged over six regions: the Pacific Northwest (PNW; 42°–48°N, 115°–125°W), California (32°–40°N, 115°–125°W), the mountain region (37°–45°N, 105°–115°W), the Ohio Valley (35°–42°N, 80°–90°W), the southern plains (32°–36°N, 90°–100°W), and Arizona and New Mexico (AZNM; 32°–36°N, 107°–113°W).

Overall, the MPDSI corresponds well to PDSI(ncdc). However, the details differ. For example, MPDSI has lower values over California during droughts in the early 1990s (Fig. 5b). Large differences also exist over the western mountain areas (Fig. 5c). Although both indices indicate long-lasting drought conditions from 2000 to 2003, the PDSI(ncdc) suggests that the drought is two or three categories more severe than that indicated by the MPDSI. The differences are likely caused by the differences in *P* and contributions from soil moisture (Figs. 4c,d). The RR assimilates *P* with the PRISM adjustment and soil moisture includes both liquid and frozen form. Over the West, *P* from the RR should be more representative. The largest discrepancy also occurs in the Ohio Valley, where the MPDSI and the PDSI(ncdc) have opposite signs from 1989 to 1990 and the MPDSI is two or three categories lower than the PDSI(ncdc) from 2000 to 2002. We will return to this point later.

The dataset is too short to study the drought duration and onset. To compare the spatial patterns of drought, composites (Fig. 6) of MPDSI and PDSI(ncdc) were made based on SPI6. SPI6 was computed based on *P* averaged over the six regions defined above. For each

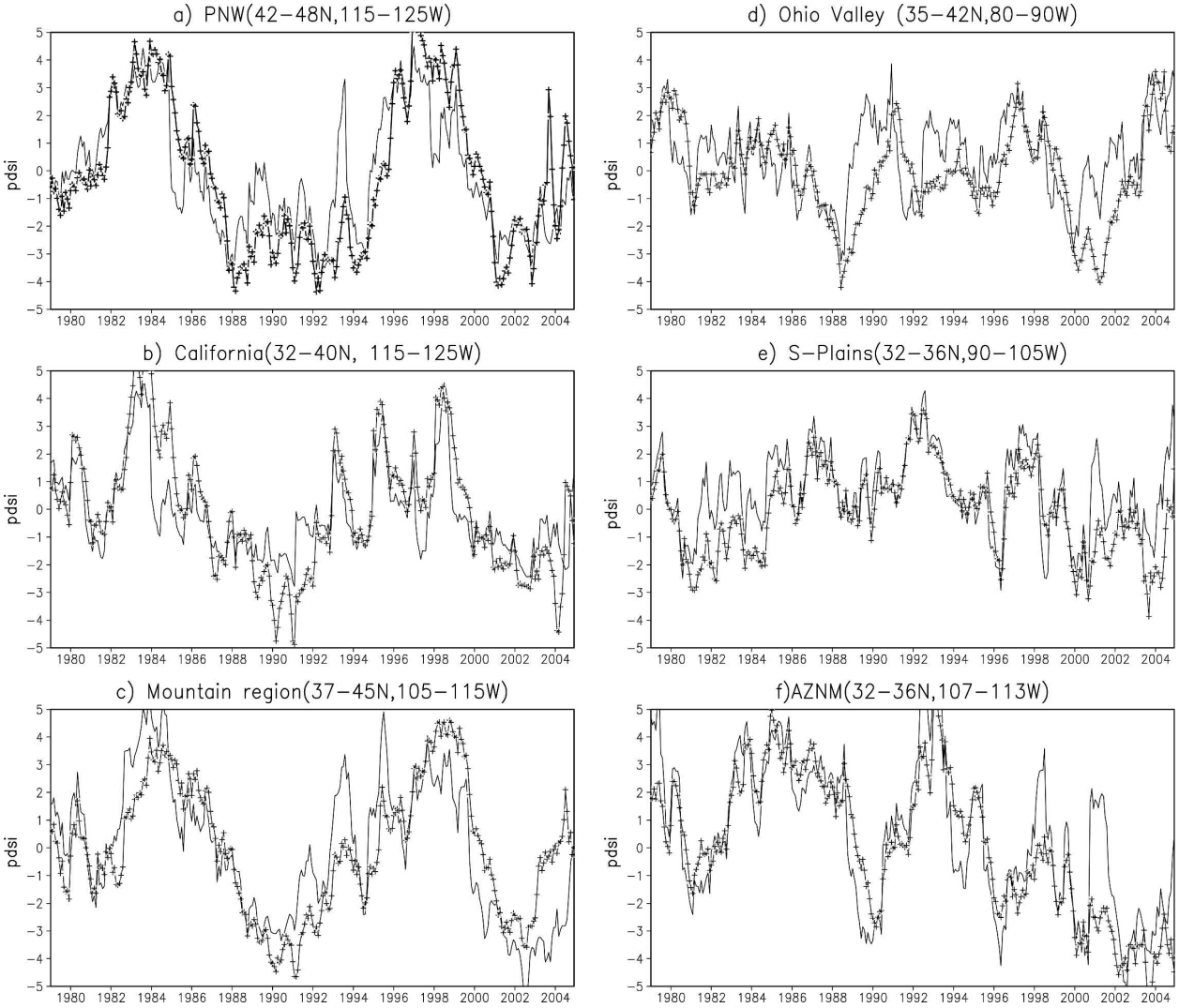

FIG. 5. The PDSI(ncdc) (solid line) and the MPDSI (plus signs) from January 1979 to December 2004, averaged over (a) the PNW (42°–48°N, 115°–125°W), (b) California (32°–40°N, 115°–125°W over land), the mountain region (37°–45°N, 105°–115°W), (d) the Ohio Valley (35°–42°N, 80°–90°W), (e) the southern plains (32°–36°N, 90°–105°W), and (f) AZNM (32°–36°N, 107°–113°W).

region, composites for MPDSI and PDSI(ncdc) for the United States were made for months for which SPI6 is below or equal −1. We counted months for which both SPI6 and MPDSI indicate drought (SPI6 is below −1 and MPDSI is below −2) at each grid point. The light (dark) shading indicates that there are more than 50% (70%) of the cases in the composite for which both the MPDSI and SPI6 indicate drought. The same shading is also applied to the PDSI(ncdc). The composites for MPDSI and PDSI(ncdc) over the Pacific Northwest, the southern plains, and the Ohio Valley are given in Fig. 6 as examples.

For the PNW, both MPDSI (Fig. 6d) and PDSI(ncdc) (Fig. 6a) indicate that drought over the PNW often spreads to Idaho. The advantage of the MPDSI's fine resolution over the mountain regions is evident (Fig. 6d). The PDSI(ncdc) is based on much coarser climate-division data (Fig. 6a) and lacks the orographically related features. The MPDSI also indicates that dryness over the Northwest is often accompanied by dryness over the Ohio Valley, consistent with the composite over the Ohio Valley (Fig. 6f).

For the southern plains, MPDSI (Fig. 6e) detects drought with values less than −2, consistent with SPI6. There are some cases in which PDSI(ncdc) (Fig. 6b) has values below −2 (light shading), but the mean is near −1, which can only be considered as mild drought. Over the Ohio Valley, both PDSI(ncdc) (Fig. 6c) and MPDSI (Fig. 6f) show drought, with indices below −2 accompanied by dryness over the West (Figs. 6d,f).

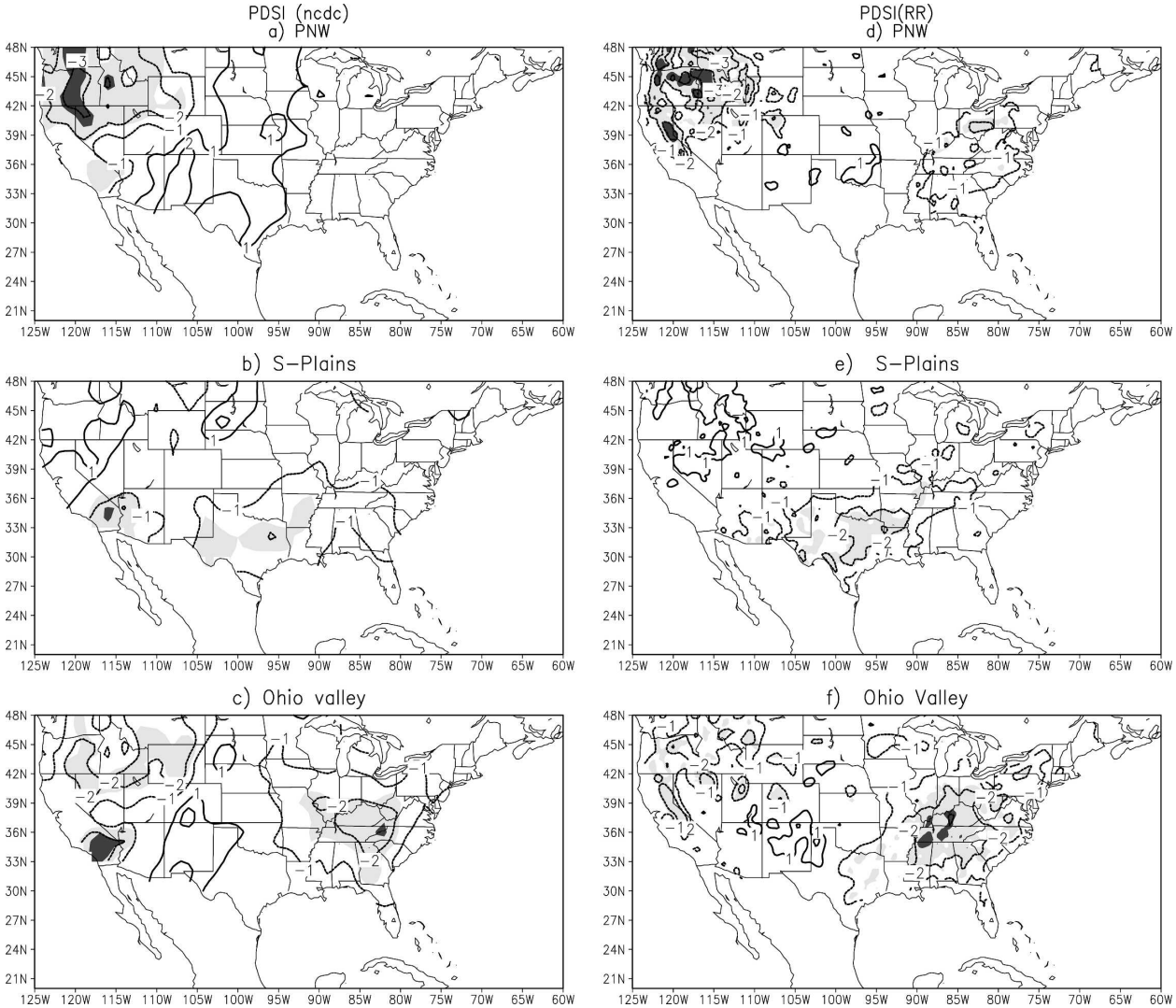

FIG. 6. Composite of the PDSI(ncdc) over drought conditions indicated by SPI6 for the (a) PNW, (b) southern plains, and (c) Ohio Valley. Contour interval is 1, with the zero contour omitted. Light (dark) shading indicates that there are more than 50% (70%) of the cases in the composite for which both the PDSI(ncdc) and the SPI6 indicate drought. (d)–(f) Same as (a)–(c), but for the MPDSI.

Overall, both indices show drought conditions over the Ohio Valley as expected. This suggests that the discrepancies between the two indices over the Ohio Valley are largely due to the wet events.

Both Fig. 5 and correlation map (Fig. 4b) show that the largest differences between the two PDSIs are over the western region and the Ohio Valley. To elaborate this point we compare the MPDSI, PDSI(ncdc), and SPI6 for the water cycle year 1990 (from October 1989 to September 1990; Fig. 7) and 2002 (from October 2001 to September 2002; Fig. 8). These two years were chosen because the largest differences between two indices over the Ohio Valley occurred in 1990 (Figs. 5 and 6) and there was an exceptionally severe drought in the western United States during 2002.

For the water cycle year 1990 over the Ohio Valley, the mean maps of both indices (Figs. 7a,d) show drought over the western states and so does the SPI6. The largest differences between two indices are that 1) the PDSI(ncdc) shows wet conditions over the Ohio Valley with PDSI greater than 2 but the wet conditions indicated by the MPDSI are confined in Georgia and 2), over the Midwest, the MPDSI shows drought over Wisconsin and Illinois, whereas the PDSI(ncdc) shows normal conditions.

The SPI6 is only 0.5 over the Ohio Valley, which does not correspond to wet events. The precipitation maps (Figs. 7e,f) both show weak anomalies and there are no large positive anomalies over the Ohio Valley. The differences over the Midwest are due mainly to the nega-

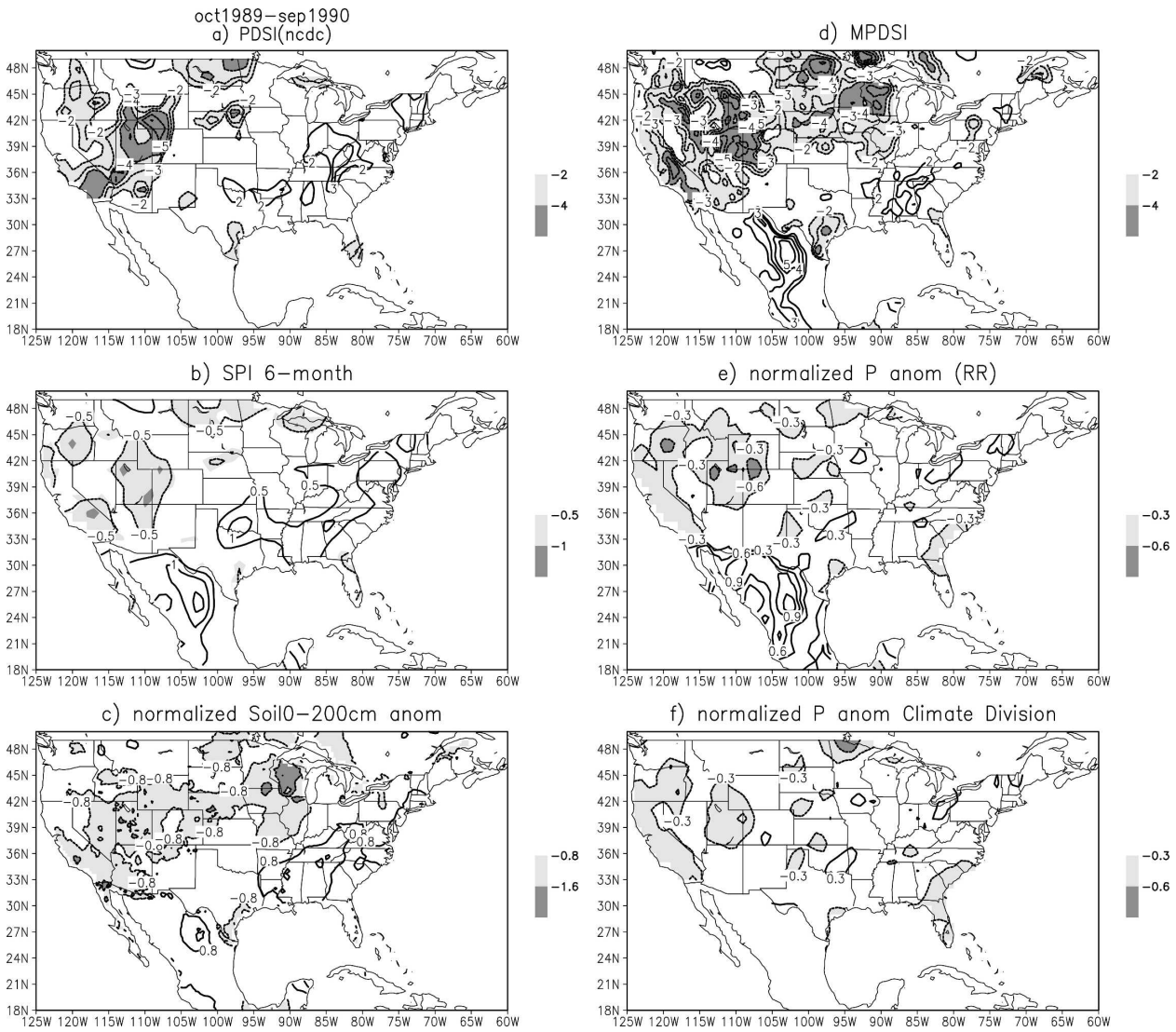

FIG. 7. (a) PDSI(ncdc) averaged for October 1989–September 1990. Contour interval is 1, with the 0, 1, and −1 contours omitted. Values less than −2 (−4) are shaded light (dark). (b) Same as (a), but for SPI6. Contour interval is 0.5. Values less than −0.5 (−1) are shaded light (dark). (c) Same as (b), but for normalized soil moisture anomaly from 0 to 200 cm. Contour interval is 0.8. Values less than −0.8 (−1.6) are shaded light (dark). (d) Same as (a), but for the MPDSI. (e) Same as (c), but for normalized precipitation anomaly from the RR. Contour interval is 0.3. Values less than −0.3 (−0.6) are shaded light (dark). (f) Same as (e), but for the normalized *P* anomaly from the climate-division data.

tive soil moisture anomalies (Fig. 7c), which contribute to higher negative MPDSI values in that region. Soil moisture anomalies also contribute to the major differences between MPDSI and PDSI(ncdc) over the Ohio Valley from June to September 1990 (not shown).

Overall for the water cycle year 2002, both indices indicate severe drought over the western United States and the eastern coastal states, separated by relative wetness over the Ohio Valley (Figs. 8a,d). The patterns are similar but the magnitudes differ. Both MPDSI and PDSI(ncdc) show severe drought extending from the Southwest to Utah, Nevada, and Oregon. The PDSI(ncdc) also shows severe drought over the Northwest, including Montana and Wyoming, whereas the MPDSI shows that these areas are already recovering from the drought conditions. Over the East Coast states, the MPDSI indicates more severe drought conditions and extends them to the Northeast up to Maine, where the values indicated by the PDSI(ncdc) are lower.

Some differences arise from the differences in precipitation. The normalized *P* anomalies from the RR

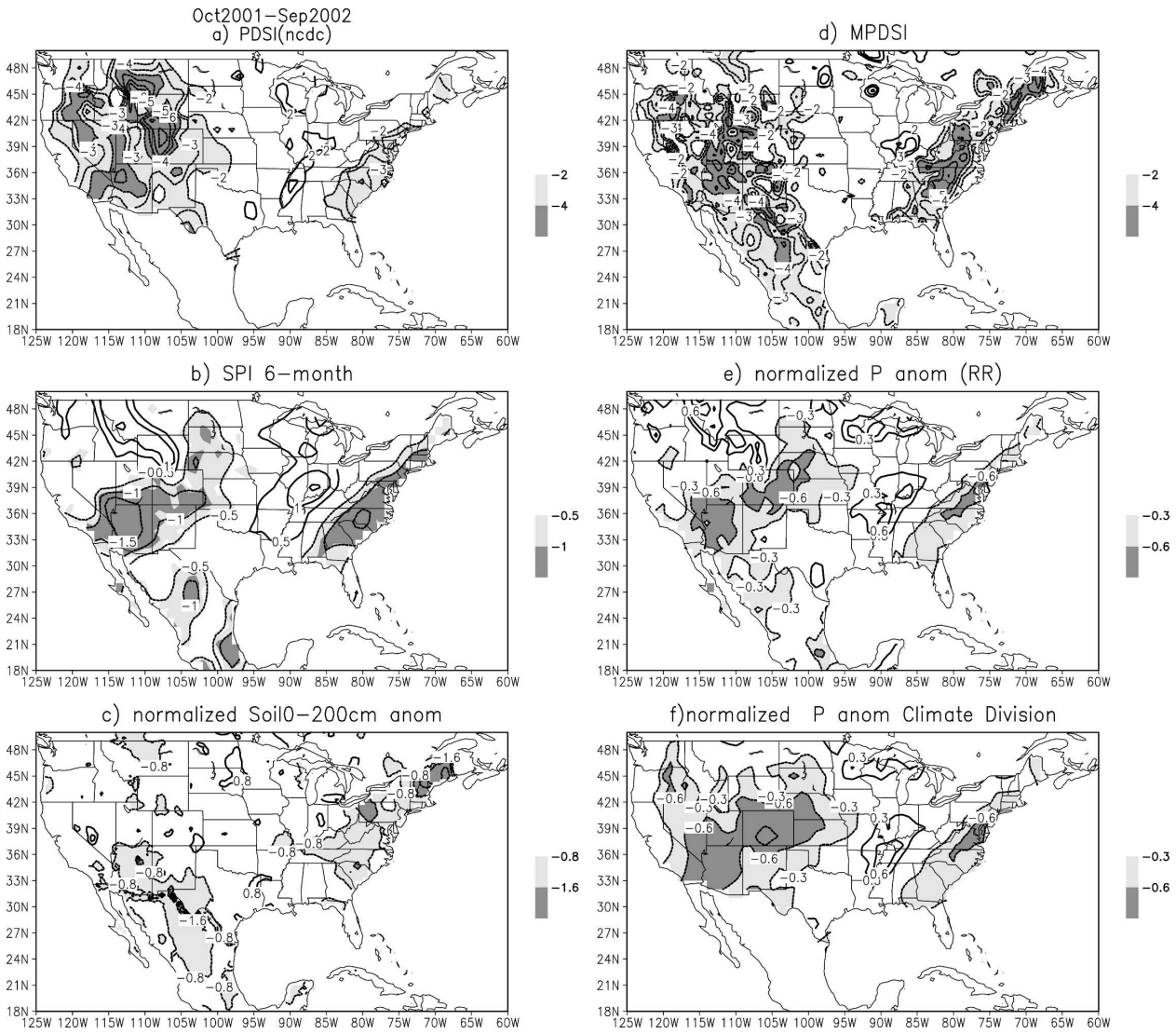

FIG. 8. Same as Fig. 7, but from October 2001 to September 2002.

and the climate-division data are shown in Figs. 8e and 8f, respectively. Both the means and standard deviations were computed using the same base period of 1979–2004. Both *P* anomalies show large negative anomalies over the Southwest and the East Coast states and positive anomalies over the Ohio Valley. The *P* anomalies from the RR (Fig. 8e) are positive over western Montana and Wyoming, consistent with the SPI6 mean (Fig. 8b). There, features are absent in the climate-division data. The *P* anomalies from the RR are close to the gauge data because the RR assimilates *P*. The MPDSI also shows more severe drought over the East Coast and extends to the Northeast where the negative soil moisture anomalies are located (Fig. 8c), because the MPDSI weights soil moisture more heavily than does the PDSI(ncdc).

4. Conclusions

We have presented a high-resolution modified Palmer drought severity index based on the North American Regional Reanalysis products. Because the original PDSI is still used in the research and agriculture community, the modified version of that index is based on the same framework as was proposed by Palmer (1965), but without the major deficiencies noted in the original index.

Many have recently questioned the very need and the utility of the original formulation of PDSI (developed using limited datasets) during an age in which more data from the NLDAS and RR are available. The PDSI is still a commonly used index for drought and is accepted in the research and agriculture community. The

PDSI(ncdc) extends to early periods when only *P* and temperature records are available. This is the major reason that we adopt many assumptions used by the PDSI. For example, the water balance equation and the difference between *P* and the climatologically expected *P* over the maximum conditions are preserved. The other assumptions invoked by Palmer (1965) are no longer needed, however. The shortcomings usually attributed to the original Palmer index as listed in the introduction are addressed in the following way in the new MPDSI:

1) Fields such as evapotranspiration, potential evapotranspiration, runoff, total soil moisture, and total soil moisture are taken directly from the RR. The Thornthwaite estimation is no longer used.
2) There is no need to use the two-layer soil model and the available water capacity. The potential recharge is defined as the total soil moisture needed to reach maximum total soil moisture at each grid point for each calendar month.
3) Because the soil moisture taken from the RR includes both solid and liquid form, the contribution of snowmelt is taken into account inexplicitly.
4) Means, maxima of variables, and normalization are now calculated separately at each grid point based on the entire dataset. Station data were not used. The RR has 32-km resolution and covers Mexico.
5) The potential precipitation is defined as the maximum precipitation at each grid point for a given calendar month. This estimation may not be the best one, but is better than using AWC. Another possibility is to estimate it from the vertically integrated moisture divergence and evaporation. The moisture fluxes are available from the atmospheric circulation and may not be available from most NLDAS products.

Overall, the MPDSI is fairly similar to the PDSI(ncdc). Because the RR has 32-km horizontal resolution, many orographically related features over the western region can now be better resolved. Because all variables are taken from the RR, they also have internal consistency. Many differences between the MPDSI and the PDSI(ncdc) arise from the differences in *P*. The RR assimilates *P* with the PRISM adjustment; therefore, *P* may be more representative than the climate-division *P*. The MPDSI also weights the contribution from soil moisture information more heavily than does PDSI(ncdc). We need to recognize that soil moisture, ET, and PE are model dependent. The MPDSI can be computed using LDAS products as along as they include the needed variables. When more NLDAS products are available, the intercomparison of the MPDSI calculated from different NLDAS products will address the uncertainties of the MPDSI. The MPDSI presented here is calculated using monthly means from the RR-based products. The calculation can also be easily extended to different time scales.

Drought is a complicated natural phenomenon and it affects people and the economy in so many different ways. Because the "same drought" implies many different things to different people, it is no wonder that it still eludes a unique definition. Hence, to monitor drought, more than one (measure) index is needed. The soil moisture at all layers, streamflow, *P*, snow information, and energetic terms are all important aspects of drought.

Acknowledgments. This work was partially supported by NOAA CPPA Grant GC06-012.

REFERENCES

Alley, W. M., 1984: The Palmer drought severity index: Limitations and assumptions. *J. Climate Appl. Meteor.,* **23,** 1100–1109.

Betts, A. K., F. Chen, K. E. Mitchell, and Z. Janjić, 1997: Assessment of the land surface and boundary layer models in two operational versions of the NCEP Eta model using FIFE data. *Mon. Wea. Rev.,* **125,** 2896–2916.

Chen, F., and Coauthors, 1996: Modeling of land surface evaporation by four schemes and comparison with FIFE observations. *J. Geophys. Res.,* **101,** 7251–7268.

——, Z. Janjić, and K. E. Mitchell, 1997: Impact of atmospheric surface layer parameterizations in the new land surface scheme of the NCEP Mesoscale Eta numerical model. *Bound.-Layer Meteor.,* **85,** 391–421.

Cosby, B. J., G. G. Homberger, R. B. Clapp, and T. R. Ginn, 1984: A statistical exploration of the relationships of soil moisture characteristics to physical properties of soils. *Water Resour. Res.,* **20,** 682–690.

Cressman, G. P., 1959: An operational objective analysis system. *Mon. Wea. Rev.,* **87,** 367–374.

Ek, M. B., K. E. Mitchell, Y. Lin, E. Rogers, P. Grunmann, V. Koran, G. Gayno, and J. D. Tarpley, 2003: Implementation of Noah land surface model advances in the National Centers for Environmental Prediction operational Mesoscale Eta Model. *J. Geophys. Res.,* **108,** 8851, doi:10.1029/2002JD003296.

Fan, Y., H. M. van den Dool, D. Lohmann, and K. Mitchell, 2006: 1948–98 U.S. hydrological reanalysis by the Noah land data assimilation system. *J. Climate,* **19,** 1214–1237.

Groisman, P. Y., R. W. Knight, T. R. Karl, D. R. Easterling, B. Sun, and J. H. Lawrimore, 2004: Contemporary changes of the hydrological cycle over the contiguous United States: Trends derived from in situ observations. *J. Hydrometeor.,* **5,** 64–85.

Hayes, M. J., M. D. Svoboda, D. A. Wilhite, and O. V. Vanyarkho, 1999: Monitoring the 1996 drought using the standardized precipitation index. *Bull. Amer. Meteor. Soc.,* **80,** 429–438.

Higgins, R. W., W. Shi, E. Yarosh, and R. Joyce, 2000: Improved

United States precipitation quality control system and analysis. *NCEP/CPC Atlas 7,* Climate Prediction Center, 47 pp.

Karl, T. R., 1983: Some spatial characteristics of drought duration in the United States. *J. Climate Appl. Meteor.,* **22,** 1356–1366.

——, 1986: The sensitivity of the Palmer drought severity index and Palmer's *Z* index to their calibration coefficients including potential evapotranspiration. *J. Climate Appl. Meteor.,* **25,** 77–86.

Koren, V., J. C. Schaake, K. E. Mitchell, Q. Y. Duan, F. Chen, and J. Baker, 1999: A parameterization of snowpack and frozen ground intended for NCEP weather and climate models. *J. Geophys. Res.,* **104,** 19 569–19 585.

Lohmann, D., and Coauthors, 2004: Streamflow and water balance intercomparisons of four land surface models in the North American Land Data Assimilation System project. *J. Geophys. Res.,* **109,** D07S91, doi:10.1029/2003JD003517.

Mahfouf, J. F., and J. Noilhan, 1991: Comparative study of various formulations of evaporation from bare soil using in situ data. *J. Appl. Meteor.,* **30,** 1354–1365.

McKee, T. B., N. J. Doesken, and J. Kleist, 1993: The relationship of drought frequency and duration to time scales. Preprints, *Eighth Conf. on Applied Climatology*, Anaheim, CA, Amer. Meteor. Soc., 179–184.

——, ——, and ——, 1995: Drought monitoring with multiple time scales. Preprints, *Ninth Conf. on Appl. Climatology,* Dallas, TX, Amer. Meteor. Soc., 233–236.

Mesinger, F., and Coauthors, 2006: North American Regional Reanalysis. *Bull. Amer. Meteor. Soc.,* **87,** 343–360.

Mintz, Y., and G. K. Walker, 1993: Global fields of soil moisture and land surface evapotranspiration derived from observed precipitation and surface temperature. *J. Appl. Meteor.,* **32,** 1305–1333.

Mitchell, K. E., and Coauthors, 2004: The multi-institution North American Land Data Assimilation System (NLDAS): Utilizing multiple GCIP products and partners in a continental distributed hydrological modeling system. *J. Geophys. Res.,* **109,** D07S90, doi:10.1029/2003JD003823.

Mo, K. C., M. Chelliah, M. Carrera, R. W. Higgins, and W. Ebisuzaki, 2005: Atmospheric moisture transport over the United States and Mexico as evaluated in the NCEP regional reanalysis. *J. Hydrometeor.,* **6,** 710–728.

Palmer, W. C., 1965: Meteorological drought. Weather Bureau Res. Paper 45, U.S. Dept. of Commerce, 58 pp.

Robock, A., and Coauthors, 2003: Evaluation of the North American Land Data Assimilation System over the southern Great Plains during the warm season. *J. Geophys. Res.,* **108,** 8846, doi:10.1029/2002JD003245.

Schaake, J. C., V. I. Koren, Q. Y. Duan, K. E. Mitchell, and F. Chen, 1996: Simple water balance model for estimating runoff at different spatial and temporal scales. *J. Geophys. Res.,* **101,** 7461–7475.

——, and Coauthors, 2004: An intercomparison of soil moisture fields in the North American Land Data Assimilation System (NLDAS). *J. Geophys. Res.,* **109,** D01S90, doi:10.1029/2002JD003309.

Shafran, P., J. Woollen, W. Ebisuzaki, W. Shi, Y. Fan, R. Grumbine, and M. Fennessy, 2004: Observational data used for assimilation in the NCEP North American Regional Reanalysis. Preprints, *14th Conf. on Applied Climatology,* Seattle, WA, Amer. Meteor. Soc., CD-ROM, 1.4.

Thornthwaite, C. W., 1948: An approach toward a rational classification of climate. *Geogr. Rev.,* **38,** 55–94.

Wells, N., S. Goddard, and M. J. Hayes, 2004: A self-calibrating Palmer drought severity index. *J. Climate,* **17,** 2335–2351.